*Biochimica et Biophysica Acta* 861 (1986) 16–24
Elsevier

BBA 73261

# A comparison of differential scanning calorimetric and Fourier transform infrared spectroscopic determination of mixing behavior in binary phospholipid systems

Joseph W. Brauner and Richard Mendelsohn

*Department of Chemistry, Newark College of Arts and Sciences, Rutgers University, 73 Warren Street, Newark, NJ 07102 (U.S.A.)*

(Received 11 March 1986)
(Revised manuscript received 9 June 1986)

Key words: Phospholipid mixture; Mixture behavior; Phase transition; Differential scanning calorimetry; Infrared spectroscopy; Fourier transform

**Fourier transform infrared (FT-IR) spectroscopy and differential scanning calorimetry (DSC) have been used to elucidate the phase behavior of two binary lipid mixtures, acyl chain perdeuterated 1,2-dipalmitoylphosphatidylethanolamine (DPPE-$d_{62}$) / 1,2-dielaidoylphosphatidylcholine (DEPC) and acyl chain perdeuterated 1,2-dipalmitoylphosphatidylcholine (DPPC-$d_{62}$) / 1,2-dimyristoylphosphatidylethanolamine (DMPE). The former shows gel state immiscibility over most of the composition range. The FT-IR data indicate that one of the solid phases is essentially pure DEPC, while the other solid phase contains both lipids. The DPPC-$d_{62}$/DMPE pair are miscible over the entire composition range. The use of deuterated lipids as one component in the mixture permits the melting characteristics of each component to be separately determined in the FT-IR experiment. The FT-IR data are used to assign the endotherms observed in the DSC to particular molecular components. For the DPPE-$d_{62}$/DEPC system, two endotherms are observed at compositions between 10 and 67 mol% DPPE-$d_{62}$. The lower transition is assigned to the DEPC component, while the higher event contains contributions to the enthalpy from both lipids in the mixture. The midpoint of the DEPC melting occurs substantially below that for DPPE-$d_{62}$. For the miscible pair, each of the lipids melt over approximately the same temperature range. The complementary and consistent nature of the information available from FT-IR and from DSC is demonstrated from the current work.**

## Introduction

Understanding the molecular basis of the interaction of membrane components remains a central focus in current biophysics (for reviews, see Refs. 1–3). We have been involved with the techniques of Fourier transform infrared (FT-IR) spectroscopy coupled with differential scanning calorimetry (DSC) toward elucidation of changes in both the dynamics and thermodynamics of lipids and proteins that occur upon their mutual interaction [4,5]. In particular, we have found it useful in reconstitution experiments to use mixtures of phospholipids where one of the molecules has its acyl chains perdeuterated. The approach permits the configuration of the acyl chains in each molecule to be monitored separately and simulta-

Abbreviations: FT-IR, Fourier transform infrared; DSC, differential scanning calorimetry; DPPE-$d_{62}$, acyl chain perdeuterated 1,2-dipalmitoylphosphatidylethanolamine; DEPC, 1,2-dielaidoylphosphatidylcholine; DMPE, 1,2-dimyristoylphosphatidylethanolamine; DPPC-$d_{62}$, acyl chain perdeuterated 1,2-dipalmitoylphosphatidylcholine.

Correspondence address: Dr. R. Mendelsohn, Department of Chemistry, Newark College of Arts and Sciences, Rutgers University, 73 Warren Street, Newark, NJ 07102, U.S.A.

0005-2736/86/$03.50 © 1986 Elsevier Science Publishers B.V. (Biomedical Division)

neously [6,7]. The configuration-sensitive C–D stretching vibrations of the perdeuterated species (2000–2200 $cm^{-1}$), appear in a spectral region distinct from the configuration-sensitive C–H spectral region (2800–3000 $cm^{-1}$) of the proteated lipid species.

The current study is an attempt to clarify the relationship between the DSC-generated endotherms for binary lipid mixtures and the FT-IR-generated melting profiles for each lipid component in the mixture. The two techniques present a complementary approach to the study of membrane structure. The lipid systems selected for the current work have different miscibility properties. The first mixture (DPPE-$d_{62}$/DEPC) is thought to have regions of both gel and fluid phase immiscibility [8], while the second mixture (DPPC-$d_{62}$/DMPE) is shown in the current work to be miscible in all proportions. The current results are essential to understand the complex and unusual protein-induced alterations observed (unpublished observation) in the reconstitution of Ca-ATPase with DPPE-$d_{62}$/DEPC mixtures.

## Experimental

*Materials*

Phospholipids (DEPC, DPPE-$d_{62}$, DMPE and DPPC-$d_{62}$) were purchased from Avanti Polar Lipids, Birmingham, AL, and were checked for purity by thin-layer chromatography and gas chromatography. The solvents used were of the highest purity commercially available. Doubly distilled water was used for all buffer solutions.

Binary lipid mixtures were made up from previously prepared stock solutions of the pure components in organic solvents. The desired ratios of binary mixtures were prepared volumetrically. Solvent was evaporated under $N_2$ gas; residual traces were removed overnight in vacuo. The dried, mixed lipids were rehydrated in 0.01 M phosphate buffer (pH 7.4). Optimal mixing was ensured by repeated vortexing at temperatures well above $T_m$ for the higher melting component.

*DSC*

DSC experiments were carried out in a Microcal MC-1 unit. Sample volumes of 0.70 ml containing 3–5 mg of the lipid suspensions dispersed in a 0.01 M phosphate buffer at pH 7.4 were injected into the sample cell. The same volume of buffer was used in the reference cell. Samples were heated at about 24 Cdeg/h following 2 h equilibration time at temperatures well below the onset of melting. Duplicate runs gave onset and peak temperatures reproducible to 0.2 Cdeg. However, the gradual nature of the breaks, especially at the completion temperatures of endothermic processes, makes it difficult to estimate their absolute values with a precision of better than $\pm 0.5$ Cdeg.

Baselines were estimated from extensions of linear regions and observations of the first significant deviations therefrom.

*FT-IR*

Samples for FT-IR contained about 10 mg of lipid dispersed in 0.01 M phosphate buffer at pH 7.4. These were placed in a Harrick cell (25 $\mu$M pathlength) equipped with $CaF_2$ or $BaF_2$ windows. Spectra were recorded on a Mattson Instruments, Sirius 100 spectrometer equipped with a liquid nitrogen-cooled HgCdTe detector. Routinely, 400 interferograms were collected, co-added, apodized with a triangular function and Fourier transformed to give about 4 $cm^{-1}$ resolution. Data were encoded every 2 $cm^{-1}$.

Temperature in the Harrick cell was controlled with a Haake FK circulating bath that circulated water through a steel block that surrounded the cell components and was monitored with a BAT-12 digital thermometer from Bailey Instruments. The thermocouple sensor was placed close to the IR windows in the cell. Temperature precision is estimated at $\pm 0.2$ Cdeg.

Spectra were solvent subtracted (solvent spectra were matched for temperature and path-length), and baseline flattened. The peak position of the C–H stretching bands were determined with a 3 point parabolic routine supplied with the instrument software. Uncertainty in the peak positions depends on the signal-to-noise ratio. Typically, in our work, 0.02–0.05 $cm^{-1}$ precision is achieved.

## Results

*I. DPPE-$d_{62}$/DEPC binary mixtures*

DSC traces for pure DEPC, pure DPPE-$d_{62}$ and for several binary mixtures of the two are

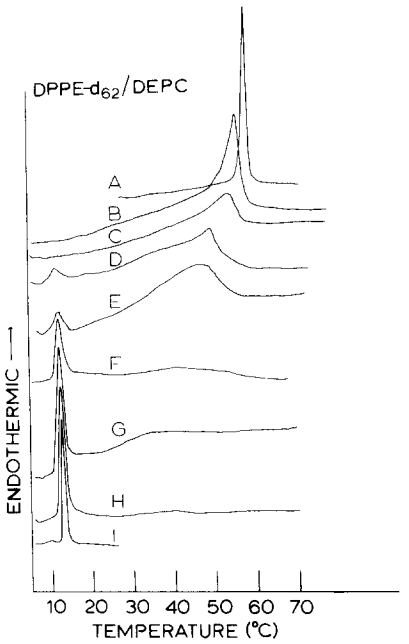


Fig. 1. DSC traces for pure DEPC, pure DPPE-$d_{62}$ and binary mixtures of the two phospholipids. The following compositions (DPPE-$d_{62}$/DEPC) are illustrated A, 100:0; B, 93:7; C, 78:22; D, 67:33; E, 49:51; F, 33:67; G, 21:79; H, 10:90; I, 0:100. The enthalpy contents are not directly comparable from trace to trace due to minor variations in scan rate and quantities of material.

shown in Fig. 1A–I. The onset, midpoint and completion temperatures for pure DEPC (Fig. 1I) are 10.7, 11.5 and 13.6°C, respectively, while for DPPE-$d_{62}$ (Fig. 1A) they are 55.0, 58.3 and 60.6°C, respectively. The width at half height for the DEPC endotherm is 0.8 Cdeg while for the DPPE-$d_{62}$ it is 1.4 Cdeg. The data for DEPC are in good accord with those of Van Dijck et al. [9] and Silvius and Gagné [10] as determined from DSC and those of Wu and McConnell [8] as determined from partitioning of a TEMPO spin label. DSC data have not been previously reported for DPPE-$d_{62}$. Acyl chain perdeuteration is seen to lower $T_m$ for this species by about five degrees, a result consistent with that for DPPC [11]. Mixing the two components at mole fractions of DPPE-$d_{62}$ from 10 to 67% results in DSC traces containing two peaks. As the mole fraction of DPPE-$d_{62}$ is increased in the mixture, the low temperature feature near 12°C is progressively diminished in intensity. At a mole fraction of 0.79 DPPE-$d_{62}$, a separate low temperature peak can no longer be distinguished. Concurrent with the progressive intensity decrease in the low temperature endotherm is the appearance at 10 mol% DPPE-$d_{62}$ and progressive enthalpy increase (with increasing DPPE-$d_{62}$) of a high temperature peak. The position of maximum intensity in the second peak increases with DPPE-$d_{62}$ content. The molecular origins of these maxima are deduced from the FT-IR data as outlined below.

The phase diagram for this lipid mixture as constructed from the set of onset and completion temperatures is plotted in Fig. 2. The horizontal line in Fig. 2 from 0 to 67 mol% DPPE-$d_{62}$ indicates regions of gel state immiscibility (phase separation) over this composition range. It is more difficult to decide whether liquid phase immiscibility occurs in this system, as suggested by Wu and McConnell [8]. Our data (Fig. 2) suggest a slight upward trend in the completion temperatures as the mole fraction of DPPE-$d_{62}$ is increased from 0.33 to 1.00, which would indicate complete miscibility in the liquid phase. However, the temperature changes are close to the limits of experimental uncertainty ($\pm$0.5 Cdeg for completion temperatures). We therefore cannot rule out, with complete confidence, a horizontal liquidus line, which would indicate immiscibility. Silvius [12] has used DSC to observe liquid phase miscibility in the DEPC/DPPE liquid mixture. The liquidus line in that study has about twice the

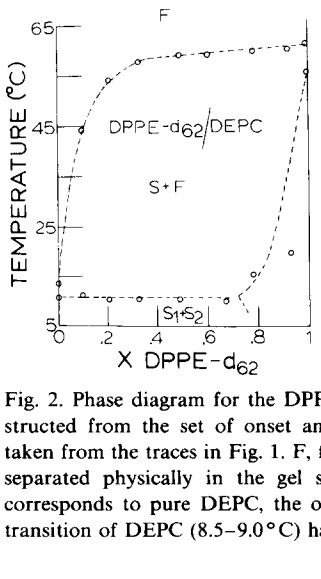


Fig. 2. Phase diagram for the DPPE-$d_{62}$/DEPC mixture constructed from the set of onset and completion temperatures taken from the traces in Fig. 1. F, fluid; S, solid. $S_1$ and $S_2$ are separated physically in the gel state. One of these phases corresponds to pure DEPC, the other is a mixture. The pretransition of DEPC (8.5–9.0°C) has been omitted.

slope over the range 0.4–1.00 mole fraction DPPE compared with our current study. Otherwise, the two investigations agree extremely well.

There are bands in the C–H stretching region of the Raman spectrum of phospholipids which might respond to changed vibrational interactions between deuterated and proteated acyl chains, hence to liquid immiscibility [13]. Preliminary investigations of these (unpublished observation) have been inconclusive.

The temperature dependence of FT-IR spectral data lend strong support to the notion of gel state phase separation in this binary mixture. Two different compositions were examined: 67:33 and 33:67 DEPC/DPPC-$d_{62}$. The C–H spectral region arising from the proteated component and the C–D stretching region of the DPPE-$d_{62}$ were examined for temperature-induced alterations in the physical state of each species. Typical spectra are shown in Fig. 3. Data at several temperatures are overlaid in Fig. 3A for the C–H stretching (2800–3000 $cm^{-1}$) region of the DEPC component and in Fig. 3B for the C–D stretching (2000–2200 $cm^{-1}$) region of the DPPE-$d_{62}$ component of a 67:33 DEPC/DPPE-$d_{62}$ mixture. Assignments of the spectral features are well established [14]. In Fig. 3A the asymmetric and symmetric $CH_3$ stretching modes appear near 2956 $cm^{-1}$ and 2872 $cm^{-1}$, respectively, while the antisymmetric and symmetric $CH_2$ stretching bands are observed at 2920 and 2850 $cm^{-1}$, respectively. A broad Fermi resonance band [15] is noted at 2900 $cm^{-1}$. The $CD_3$ groups of the DPPE-$d_{62}$ (Fig. 3B) give rise to bands at 2212 $cm^{-1}$ (asymmetric stretch) and at 2169 and 2070 $cm^{-1}$ (symmetric stretch), while the stronger bands near 2195 and 2090 $cm^{-1}$ are the antisymmetric and symmetric $CD_2$ stretching modes, respectively [14]. Changes in the position and intensity of the bands have been used (for a review, see Ref. 16) to follow the melting of each lipid component.

Melting curves for each lipid component constructed from the data in Fig. 3 are displayed in Fig. 4. For the DEPC constituent (Fig. 4A), the temperature dependence of the symmetric $CH_2$ stretching vibration near 2850 $cm^{-1}$ is the parameter monitored. The increase in frequency as temperature is raised is due to alterations in the interaction constants between C–H stretching co-

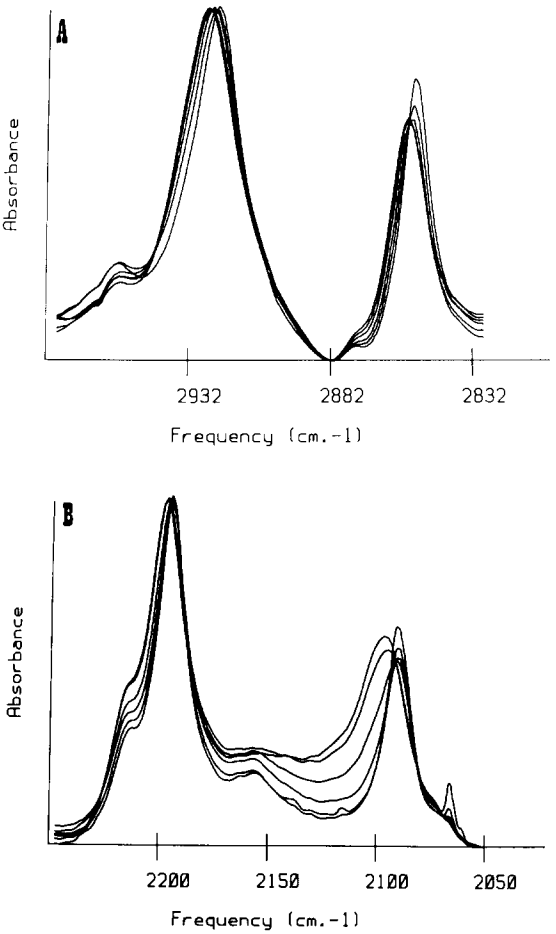


Fig. 3. A. The C–H stretching region of the FT-IR spectrum of a DEPC/DPPE-$d_{62}$ 67:33 binary mixture. Data at several temperatures are overlaid. In general, peak heights decrease and frequencies increase with increasing temperature. The rapid variation in the initial scans suggests that the DEPC component being monitored here has a rapid melting fraction. Data are plotted at about 5 Cdeg temperature intervals between 2 and 70°C. B, the C–D stretching region of the FT-IR spectrum of a DEPC/DPPE-$d_{62}$ 67:33 binary mixture. Data at several temperatures are overlaid as in A. The rapid variation in spectral parameters occurs at much higher temperatures than for the DEPC component of the sample.

ordinates on adjacent $CH_2$ groups when gauche rotamers are formed [17]. A sharp discontinuity with a magnitude of about 0.5 $cm^{-1}$ is observed in Fig. 4A between 11 and 13°C, close to the melting of pure DEPC (see the DSC data in Fig. 1). In addition, a non-cooperative process persists until about 40°C, at which point the variation with temperature in the plotted spectral parameter be-

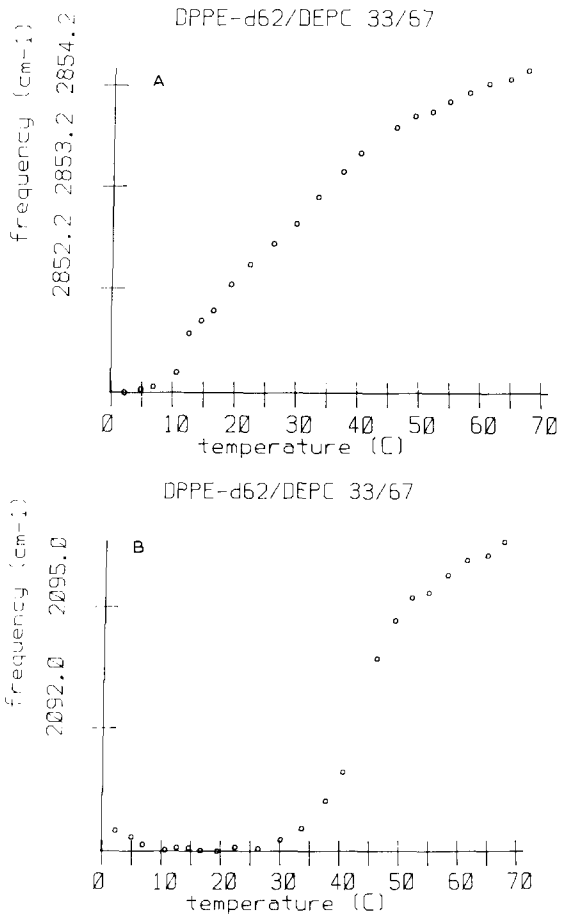


Fig. 4. Melting curves for each lipid component in a 67:33 DEPC/DPPE-$d_{62}$ binary mixture as constructed from FT-IR data. A, the temperature dependence of the symmetric $CH_2$ stretching vibration arising primarily from the DEPC is shown. B, the temperature dependence of the symmetric $CD_2$ stretching vibration arising from the DPPE-$d_{62}$ component is shown.

comes much less rapid. These data are consistent with the existence (as deduced from DSC) of a separate phase of DEPC in the system which melts at the temperature of the pure material. It is important to note that not all the DEPC exists as a separate solid phase. The observation of the non-cooperative component persisting until substantially higher temperatures suggests that a substantial fraction of this component is mixed in domains with DPPE-$d_{62}$ and hence has its phase transition temperature increased. At 79 mol% DPPE-$d_{62}$, no pure phase of DEPC can be detected in the DSC trace (Fig. 1). Thus, the composition of the two solid phases (in the region of phase separation) consists of a pure DEPC phase and a phase containing both lipid components in proportions depending on the composition. There is no distinct DPPE-$d_{62}$ phase.

Melting of the DPPE-$d_{62}$ component in the sample is conveniently monitored (Fig. 4B) from a plot of the temperature-induced variation in the $CD_2$ antisymmetric stretching frequency near 2090 $cm^{-1}$. A broad melting event is observed over the temperature range 30–53°C. The substantial increase in the melting range and lowering of the transition temperature suggests the strong interac-

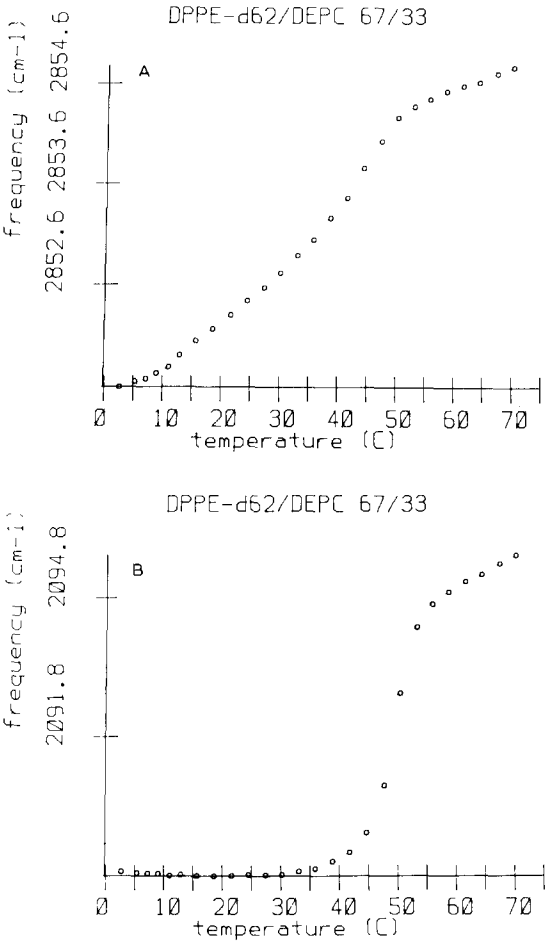


Fig. 5. Melting curves for each lipid component in a 33:67 DEPC/DPPE-$d_{62}$ binary mixture, as constructed from FT-IR data. A, the temperature dependence of the symmetric $CH_2$ stretching vibration arising primarily from the DEPC is shown. B, the temperature dependence of the symmetric $CD_2$ stretching vibration arising from the DPPE-$d_{62}$ component is shown.

tion between components in this system, a result consistent with observations of the DEPC fraction.

The thermotropic behavior of the components in a 33:67 DEPC/DPPC-$d_{62}$ sample are shown in Fig. 5. The independent melting of the two components is again well illustrated. The DEPC component (Fig. 5A) exhibits a very weak inflection at 12–15°C, and an additional gradual melting event which terminates near 50°C. The DPPE-$d_{62}$ melts fairly cooperatively between 45 and 55°C (Fig. 5B). Melting curves for the pure components constructed for FT-IR data (not shown) demonstrate phase transitions at approx. 12°C for DEPC and approx. 58°C for DPPE-$d_{62}$. No significant increases in peak frequencies are observed above $T_m$.

*II. DMPE / DPPC-$d_{62}$ binary mixtures*

DSC traces for pure DMPC, pure DPPC-$d_{62}$ and various binary mixtures are shown in Fig. 6. The onset, midpoint and completion temperatures for the DMPE occur at 47.5, 49.7, and 51.0°C, respectively, while for the DPPC-$d_{62}$, they appear at 33.0, 35.7 and 39.2°C. Pure DPPC-$d_{62}$ also

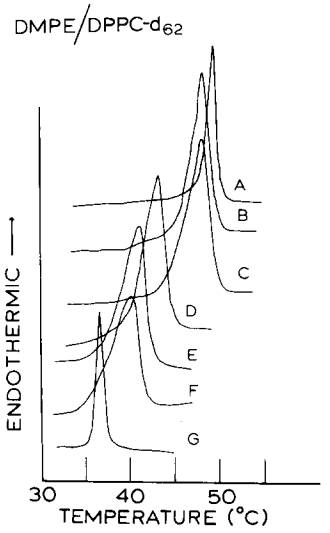


Fig. 6. DSC traces for pure DMPE, pure DPPC-$d_{62}$ and binary mixtures of the two phospholipids. The following compositions (DMPE/DPPC-$d_{62}$) are illustrated: A, 100:0; B, 80:20; C, 67:33; D, 50:50; E, 33:67; F, 20:80; and G, 0:100. As in Fig. 1, enthalpies are not directly comparable from sample to sample.

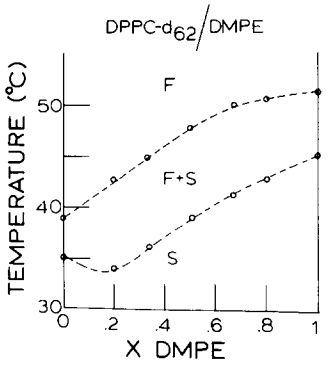


Fig. 7. Phase diagram for the DMPE/DPPC-$d_{62}$ mixture constructed from the collection of onset and completion temperatures of the data shown in Fig. 6. The lack of a horizontal region in the solidus line suggests that the lipids are miscible throughout the diagram.

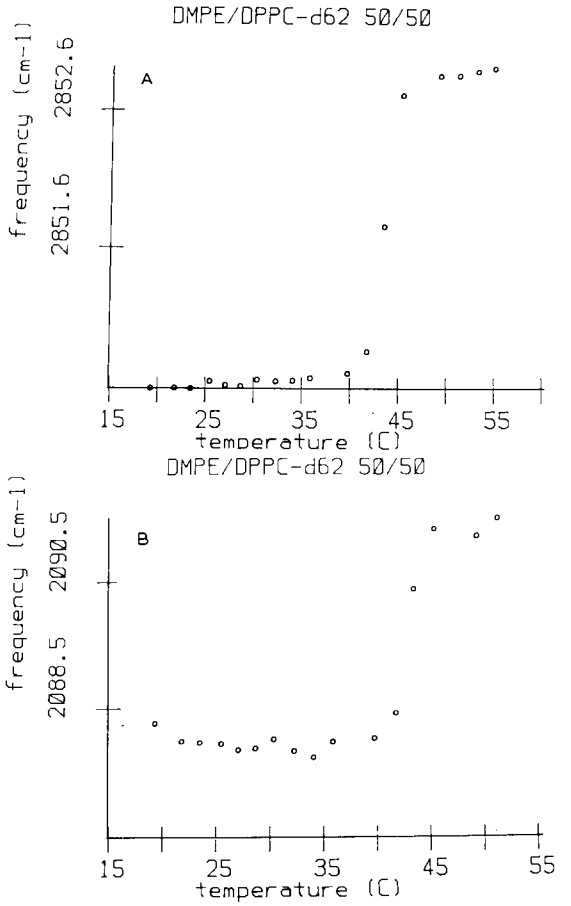


Fig. 8. Melting curves for each lipid component in a 50:50 DMPE/DPPC-$d_{62}$ binary mixture as constructd from FT-IR data. A, the temperature dependence of the $CH_2$ symmetric stretching vibration arising from the DMPE component is shown. B, the temperature dependence of the symmetric $CD_2$ stretching vibration arising from the DPPC-$d_{62}$ component is shown.

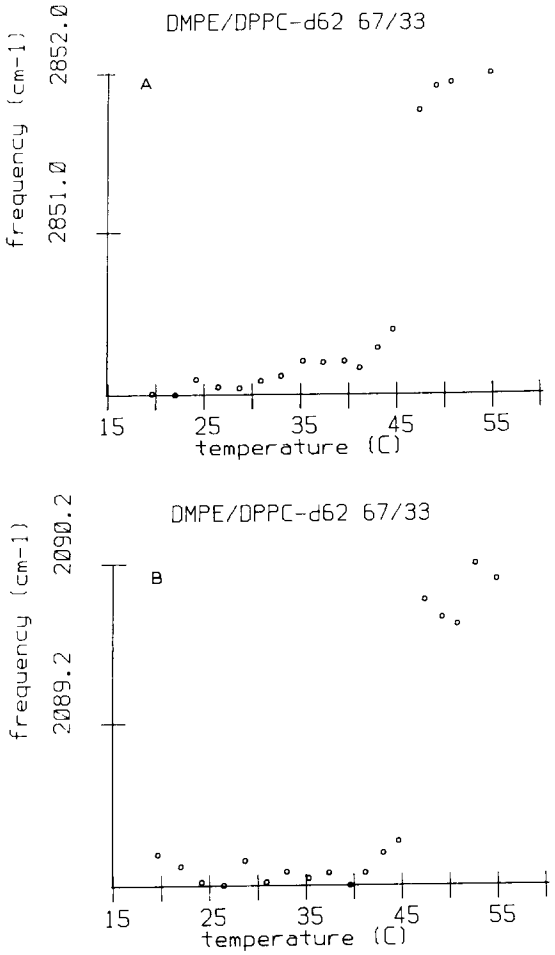


Fig. 9. Melting curves for each lipid component in a 67:33 DMPE/DPPC-$d_{62}$ binary mixture as constructed from FT-IR data. A, the temperature dependence of the $CH_2$ symmetric stretching vibration arising from DMPE. B, the temperature dependence of the symmetric $C^2H_2$ stretching vibration arising from DPPC-$d_{62}$.

exhibited a weak pretransition endotherm (data not shown) between 25 and 27°C. Addition of small amounts (10%) of DMPE abolished this event. We have omitted pre-transitions from the phase diagram. A single, broadened endothermic peak is noted for the binary mixtures at all compositions, with asymmetry (shoulders) being evident in some of the traces. The phase diagram is given in Fig. 7. The diagram indicates lipid miscibility over the entire range of composition although non-ideal behavior is evident. Similar data (for the lipid pair with proteated chains on each species) were obtained by Blume and Ackermann [18], although their interpretation of the phase diagram was different. In the current interpretation, the absence of substantial horizontal regions in the solidus line is interpreted as indicating the absence of gel state phase separation.

The FT-IR melting characteristics for each component of two binary mixtures with compositions 50:50 and 67:33 DMPE/DPPC-$d_{62}$ are displayed in Figs. 8 and 9. The melting patterns shown for each lipid differ dramatically from those observed for the DEPC/DPPE-$d_{62}$ pair. For each composition of this mixture that was studied, the two components exhibit the same melting profile. In Fig. 8, where data are shown for a 50:50 mixture, each component is seen to melt between 40 and 46°C in good accord with the DSC data (Fig. 7). In Fig. 9, the data are shown for a 67:33 (DMPE/DPPC-$d_{62}$) sample. In this instance, each component shows a slight frequency increase between 40 and 45°C, followed by a rapid increase in frequency over the next degree or two. The similarity in the melting of each component is consistent with their miscibility over the entire range of compositions, in good accord with the DSC data.

## Discussion

The current experiments demonstrate the complementary nature of the information available from FT-IR and from DSC. The FT-IR experiment directly (without the use of a probe molecule) identifies the molecular components which take part in the calorimetric endothermic events. Furthermore, the technique is equally well able to monitor broadened transitions or cooperative melting processes. It is noted that perdeuterated lipids are not always required for identification of a particular component. Certain lipid types will have characteristic bands. In the current work for example, the DEPC component has a C–H in-plane bending mode near 960 $cm^{-1}$, characteristic of *trans* C=C bonds. Similar modes exist for *cis* C=C containing lipids and additional characteristic vibrations can be anticipated for polyunsaturated chains.

DSC data unambiguously define thermodynamic functions for the melting. However, the

method cannot identify molecular species, nor can it easily follow low enthalpy, non-cooperative processes. In complex environments such as native membranes, these are likely to dominate.

Comparison of the methods is facilitated by examination of the derivative of the FT-IR melting curves and the DSC data as shown in Figs. 10 and 11 for the two binary lipid mixtures of DEPC/DPPE-$d_{62}$ used in the FT-IR experiments. The infrared data for the 67:33 binary mixture demonstrate (Fig. 10B and C) some scatter in the points and illustrate the necessity for high quality FT-IR spectral data. A comparison of the three curves is instructive. First, the low temperature endotherm in the DSC trace (Fig. 10A) clearly arises from the DEPC component whose FT-IR melting (Fig. 10B) occurs sharply at the data point nearest 12°C. Second, the broad, barely detectable endotherm which extends from 29°C till about 54°C has contributions from both lipids. The DPPE-$d_{62}$ (Figs. 4 and 10C) melts over a range from 30 to 53°C, with a maximum rate of change at 41°C, close to the maximum of the high temperature endotherm. In addition to the sharp melt, the DEPC (Fig. 10B) melts non-cooperatively until about 40–45°C, and clearly contributes to the calorimetric maximum. The data, when plotted in the current fashion, help to assign the broad, weak, high temperature endotherm to those species

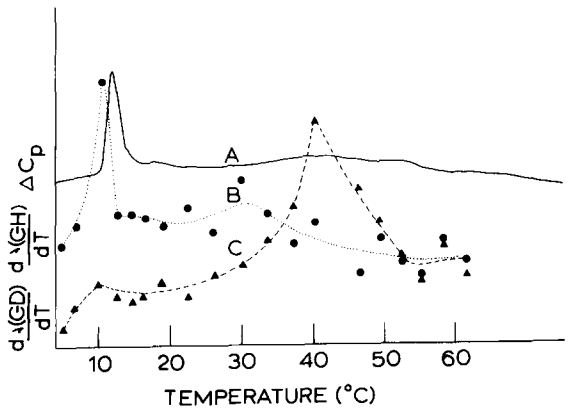


Fig. 10. A detailed comparison of DSC and FT-IR data for the 67:33 DEPC/DPPE-$d_{62}$ system. A, DSC data. B, the derivative of the melting curve of the C–H component, i.e., the data shown in Fig. 4A. C, the derivative of the melting curve of the C–D component, i.e., the data shown in Fig. 4B. The amplitudes of the various ordinate scales are definitely not comparable.

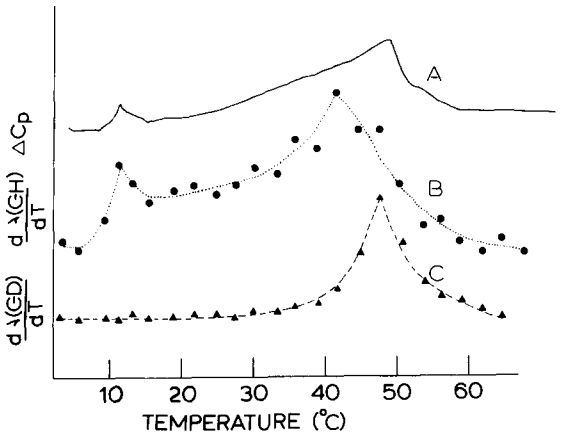


Fig. 11. A detailed comparison of DSC and FT-IR data for the 33:67 DEPC/DPPE-$d_{62}$ system. A, DSC data; B, the derivative of the melting curve of the C–H component, i.e., the data shown in Fig. 5A; C, the derivative of the melting curve of the C–D component, i.e., the data shown in Fig. 5B. The amplitudes of the various ordinate scales are definitely not comparable.

responsible for the melting event.

Similar patterns are seen for the 33:67 mixture (Fig. 11). The inflection in the FT-IR melting curve for the DEPC component at about 12°C (Fig. 5A), is seen both in the DSC data (Fig. 11A) and as a more intense feature in the IR derivative plot for DEPC (Fig. 11B). The broad transition seen in the DSC between 22 and 60°C clearly contains contributions from both DEPC and DPPE-$d_{62}$. Each has a maximum at its own temperature – the DEPC at 40°C, the DPPE-$d_{62}$ at 48°C.

FT-IR and DSC thus give consistent and complementary views of lipid mixing characteristics for this phase-separated system. The use of the derivative plots (Figs. 10 and 11) is helpful in correlating the two techniques. The observation of distinct domains containing some, but not all of the DEPC in the DPPE-$d_{62}$/DEPC system is evident for gel state phase separation of the system, a result consistent with the DSC. For the DPPC-$d_{62}$/DMPE system, the coincidence of the melting of the two components as judged by FT-IR is consistent with, but does not independently prove, the miscibility of this lipid pair. Mixtures with a eutectic would behave in similar fashion, especially at compositions close to the eutectic.

FT-IR is most useful under conditions where

DSC data cannot easily be acquired, i.e., where the transitions are broadened (in the presence of protein, for example [7]), or where the enthalpies are small. We have also used the technique to observe the existence of gel phase domains in phospholipid vesicles reconstituted with Ca-ATPase [5]. Extensions to native systems, including those into which deuterated lipids have been incorporated, appear feasible. Encouraging data along these lines have been reported [19].

## Acknowledgements

This study was supported by a grant to R.M. from the US National Institutes of health (GM 29864). Additional support from the Busch bequest of Rutgers University is acknowledged. We would like to thank Professor John Silvius of McGill University for a preprint of his manuscript (Ref. 12).

## References

1 Gennis, R.B. and Jonas, A. (1977) Annu. Rev. Biophys. Bioeng. 6, 195–238
2 Parsegian, A. (ed.) (1982) Biophysical Discussions; Protein-Lipid Interactions in Membranes, Rockefeller University Press
3 Gruner, S.M., Cullis, P.R., Hope, M.J. and Tilcock, C.P.S. (1985) Ann. Rev. Biophys. Biophys. Chem. 14, 211–238
4 Mendelsohn, R., Anderle, G., Jaworsky, M., Mantsch, H.H. and Dluhy, R.A. (1984) Biochim. Biophys. Acta 775, 215–224
5 Jaworsky, M. and Mendelsohn, R. (1986) Biochim. Biophys. Acta 860, 491–502
6 Dluhy, R.A., Moffatt, D., Cameron, D.G., Mendelsohn, R. and Mantsch, H.H. (1985) Can. J. Chem. 63, 1925–1932
7 Jaworsky, M. and Mendelsohn, R. (1985) Biochemistry 24, 3422–3428
8 Wu, S.H.W. and McConnell, H.M. (1975) Biochemistry 14, 847–854
9 Van Dijck, P.W.M., Kaper, A.J., Oonk, H.A.J. and De Gier, J. (1977) Biochim. Biophys. Acta 470, 58–69
10 Silvius, J.R. and Gagné, J. (1984) Biochemistry 23, 3241–3247
11 Klump, H.H., Gaber, B.P., Peticolas, W.L. and Yager, P. (1981) Thermochim. Acta 48, 361–366
12 Silvius, J. (1986) Biochim. Biophys. Acta 857, 217–228
13 Mendelsohn, R. and Maisano, J. (1978) Biochim. Biophys. Acta 506, 192–201
14 Cameron, D.G., Casal, H.L., Mantsch, H.H., Boulanger, Y. and Smith, I.C.P. (1981) Biophys. J. 35, 1–16
15 Snyder, R.G., Hsu, S.L. and Krimm, S. (1978) Spectrochim. Acta, Part A 34, 395–406
16 Mendelsohn, R. and Mantsch, H.H. (1986) in Progress in Protein-Lipid Interactions 2 (Watts, A. and De Pont, J.J.H.H.M., eds.), pp. 103–146, Elsevier Science Publishers
17 Snyder, R.G., Strauss, H.L. and Elliger, C.A. (1982) J. Phys. Chem. 86, 5145–5150
18 Blume, A. and Ackermann, T. (1974) FEBS Lett. 43, 71–74
19 Cameron, D.G., Martin, A., Moffatt, D.J. and Mantsch, H.H. (1985) Biochemistry 24, 4355–4359